SCIENTIFIC REPORTS

OPEN

SUBJECT AREAS:
STRUCTURE OF SOLIDS AND LIQUIDS
ELECTRONIC DEVICES
SUPERCONDUCTORS
SUPERCONDUCTING PROPERTIES AND MATERIALS

Received
3 December 2012

Accepted
8 February 2013

Published
15 March 2013

Correspondence and requests for materials should be addressed to S.L. (stefano.leoni@chemie.tu-dresden.de)

Novel metastable metallic and semiconducting germaniums

Daniele Selli[1], Igor A. Baburin[1,2], Roman Martoňák[3] & Stefano Leoni[1]

[1]Technische Universität Dresden, Institut für Physikalische Chemie, 01062 Dresden, Germany, [2]Max-Planck-Institut für Chemische Physik fester Stoffe, 01187 Dresden, Germany, [3]Department of Experimental Physics, Comenius University, Mlynská Dolina F2, 842 48 Bratislava, Slovakia.

Group-IVa elements silicon and germanium are known for their semiconducting properties at room temperature, which are technologically critical. Metallicity and superconductivity are found at higher pressures only, Ge *β*-tin (tI4) being the first high-pressure metallic phase in the phase diagram. However, recent experiments suggest that metallicity in germanium is compatible with room conditions, calling for a rethinking of our understanding of its phase diagram. Missing structures can efficiently be identified based on structure prediction methods. By means of *ab initio* metadynamics runs we explored the lower-pressure region of the phase diagram of germanium. A monoclinic germanium phase (mC16) with four-membered rings, less dense than diamond and compressible into *β*-tin phase (tI4) was found. Tetragonal bct-5 appeared between diamond and tI4. mC16 is a narrow-gap semiconductor, while bct-5 is metallic and potentially still superconducting in the very low pressure range. This finding may help resolving outstanding experimental issues.

The fundamental character and technological relevance of group-IVa elements (tetrels) have motivated repeated investigations and systematics on their polymorphism[1–5]. Carbon polymorphs are promising as hard and transparent materials[6,7]. Semiconducting silicon (Si) is versatile for micro- and nanoelectronic devices, while germanium (Ge) displays comparatively higher carrier mobility, a finer band gap tunability, and good compatibility with high-dielectric constant materials[8]. Metallization occurs in silicon and germanium upon compression[1]. In Ge lowering of phonon frequencies promotes electron-phonon coupling towards superconductivity[2,3]. The possibility of metallic germanium under room conditions is very intriguing and intensively debated[2,9], while superconductivity in elemental Ge appears under pressure[3]. In the lower pressure range, improved optical properties via band-gap tuning can be achieved in a different polymorph.

Engineering viable new compounds with superior properties entails a detailed understanding of structural changes[10]. Under pressure germanium bears similarities with silicon[1] by comparatively higher transition pressures with respect to Si, due to Ge core d-electrons[11]. Upon compression semiconducting Ge (cubic diamond) transforms into β-tin type (space group $I4_1/amd$) at about 10 GPa[12], and then to Imma phase[13], simple hexagonal (P6/mmm)[14], followed by orthorhombic Cmca phase[15] and finally upon further compression above 180 GPa, by the hexagonal close-packed arrangement ($P6_3/mmc$)[15].

The phase diagram of germanium is further complicated by a family of tetrahedral structures[16,17]. Type-II clathrate Ge(cF136) exists at ambient conditions[17]. Other germanium modifications are reported, Ge(tP12), Ge(cI16) (γ-silicon type, BC8) and Ge(hR8)[16]. BC8 Ge[18] is accessible through decompression from β-tin Ge. In a nutshell, during the last few years, new dense and open phases of germanium have been experimentally observed or synthesized. Nevertheless, a systematic approach to including known and finding novel germanium forms is still outstanding, and of top priority in order to explain recent experiments[2].

In this work we explore the energy landscape of germanium, both at ambient conditions and upon moderate compression. By means of *ab initio* metadynamics, we efficiently sampled structural transformations along appropriate collective reaction coordinates. Besides the already known dense phases of germanium, we found two novel allotropes (green in Fig. 1). The first one is a monoclinic modification of germanium (mC16) slightly less dense than diamond, is an indirect band gap semiconductor and is unprecedented for tetrel elements. The second one is a five-coordinated (square pyramidal) metallic intermediate structure (tI4, sp. gr. I4/mmm), which incurs in the diamond (cF8) $\rightarrow$ β-tin phase (tI4) transition, and which has been postulated to exist in homologue silicon (bct-5)[19]. We report on transformation paths, energetic, mechanical and electronic properties. For the metallic bct-5 phase, we calculated superconducting temperatures down to ambient pressure compared to β-tin phase, based on the electron-phonon coupling mechanism[20].

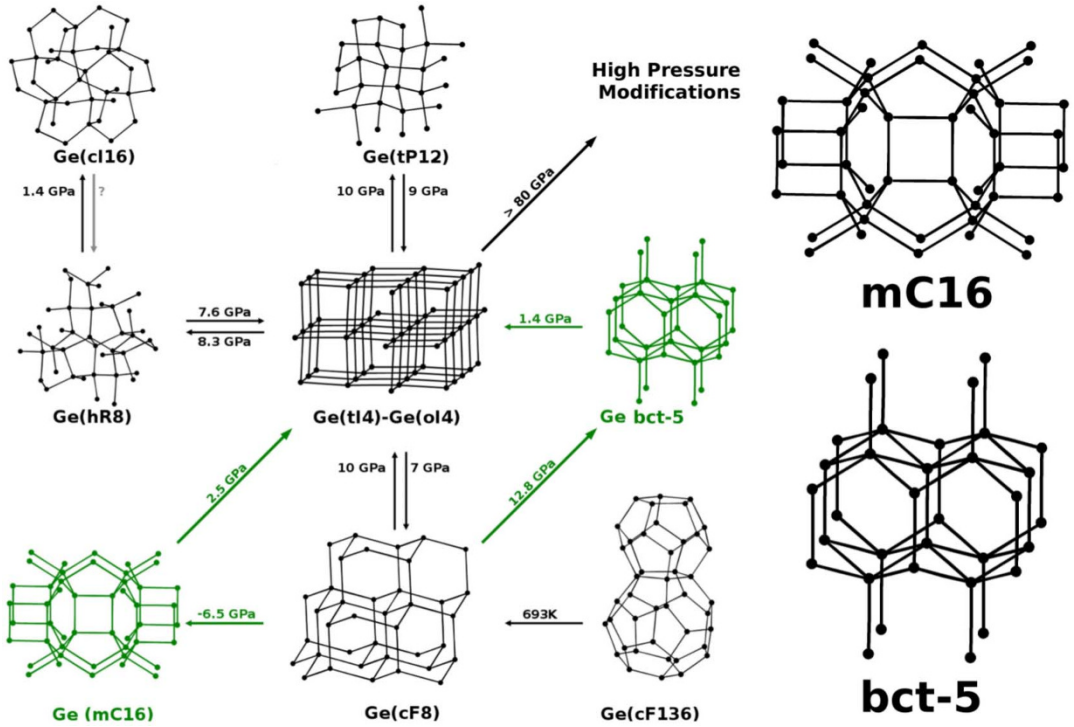

Figure 1 | Lower pressure region of the phase diagram of Ge, augmented by two novel phases mC16 and bct-5, found by *ab initio* metadynamics runs. bct-5 shows characteristic square pyramidal 5-fold coordination of Ge atoms. In monoclinic mC16 four-rings are a characteristic feature. The arrows indicate the direction of metadynamics evolution. The pressures were evaluated based on the common tangent construction (see below, Fig. 2).

Results

The mC16 structure (Fig. 1, C2/m, $a = 7.6094$ Å, $b = 7.9746$ Å, $c = 6.5668$ Å, $\beta = 104.10^{\circ}$) arised from a metadynamics run started from diamond (8 atoms box, $p = 1$ bar, $T = 300$ K). Ge atoms occupy three Wyckoff positions: (4*i*) 0.70984 0.50000 0.67434, (4*i*) 0.60981 0.50000 0.29080, (8*j*) 0.65012 0.76388 0.11596. Strikingly, mC16 is less dense than diamond (see Fig. 2), although topologically as dense as diamond or lonsdaleite. Its bulk modulus amounts to 51.2 GPa that is slightly lower than that of the diamond type-structure (60.7 GPa), estimated from the fit to the third order Birch-Murnaghan equation of state. Applying pressure to the mC16 allotrope in an additional metadynamics run resulted into a direct transition to the β-tin phase. Decompressing the latter is known to generate metastable phases typically denser than diamond Ge.

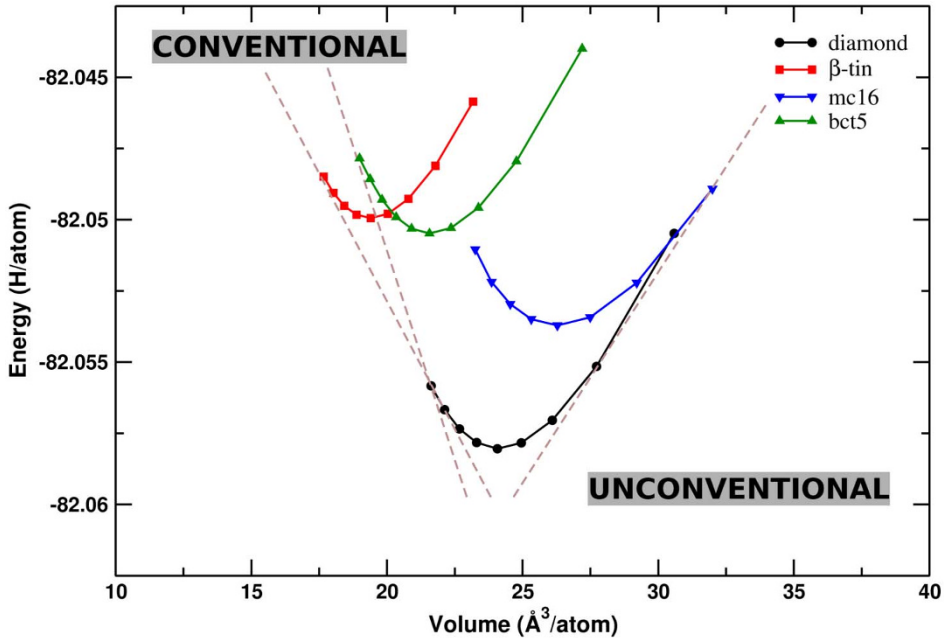

Figure 2 | Equation of states of Ge mC16 and bct-5, compared to cubic diamond and β-tin type. bct-5 features a reduced volume per atom compared to diamond type (cF8), while the total energy minimum lies lower than β-tin. mC16 on the contrary is less dense and energetically close to the diamond type. The tangents used for evaluating equilibrium pressures of Fig. 1 are highlighted.

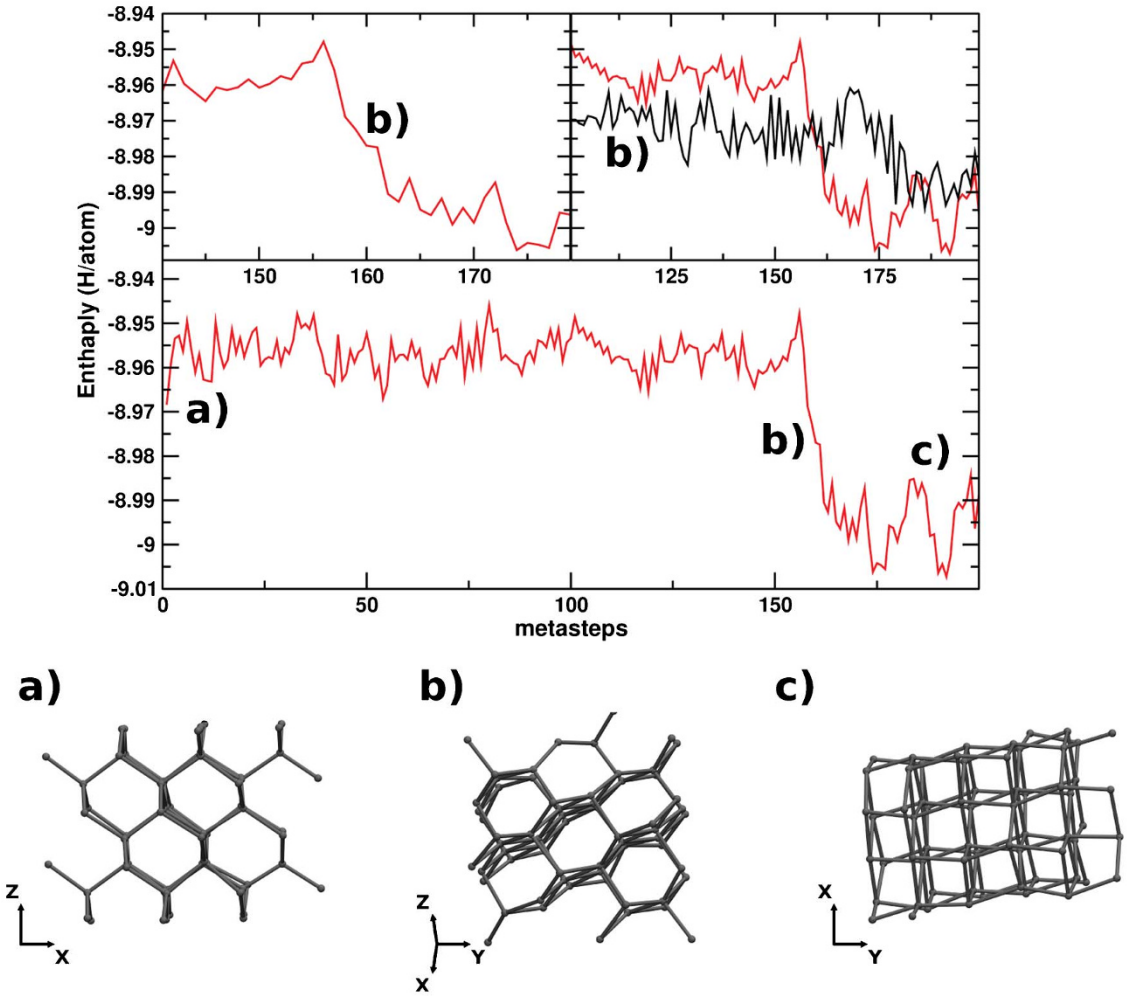

Figure 3 | Metadynamics (DFT) runs on a 64 Ge atoms box (p_1 = 10.0 GPa, T = 300 K). bct-5 appears as a stepwise feature in the enthalpy profile of the run started from diamond (red line). Runs commenced from bct-5 (black line) evolve into β-tin. Configurations corresponding to distinct points along the runs are detailed below the graph. Energy units are eV.

Therefore, a viable route to mC16, like for other recent germanium allotropes, could rather be the oxidation of suitable germanium Zintl salt precursors, i.e. via chemical synthesis.

Upon compression diamond transforms into β-tin and it subsequently follows the same transition sequence of silicon phases. Along the diamond → β-tin transition metadynamics (64 atoms box, p = 10 GPa, T = 300 K, Gaussian width δs = 4.5 (GPa Å^3)$^{(1/2)}$, Gaussian height W = δs^2) visited an intermediate of bct-5 topology (I4/mmm, a = 3.5491, c = 6.4478, Ge(4e) 0.0 0.0 0.19273). The bct-5 bulk modulus is 58.7 GPa, slightly lower than that of the β-tin phase (68.2 GPa). This five-connected structure has been proposed for silicon[19], but has never been observed so far.

The total energy/volume curves of Fig. 2 suggest bct5 as a conventional product of diamond compression (here "conventional" denotes a positive equilibrium pressure, whereby an "unconventional" product requires a "negative" pressure). However, under hydrostatic conditions β-tin is formed from diamond, while decompression leads to other germaniums, although indications of minority

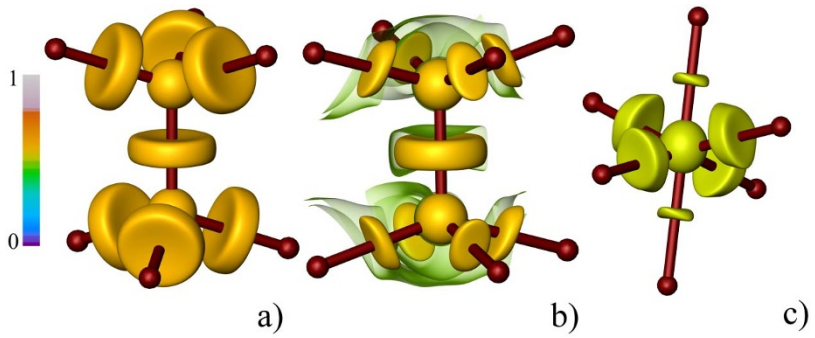

Figure 4 | Evolution of the bonding situation from diamond to β-tin type over bct-5. The ELF map is showing four bond attractors for diamond Ge (a, η = 0.58), one + four bond attractors for bct-5 (b, η = 0.53, transparent green isosurface η = 0.48), two + four bond attractors for β-tin (c, η = 0.51).

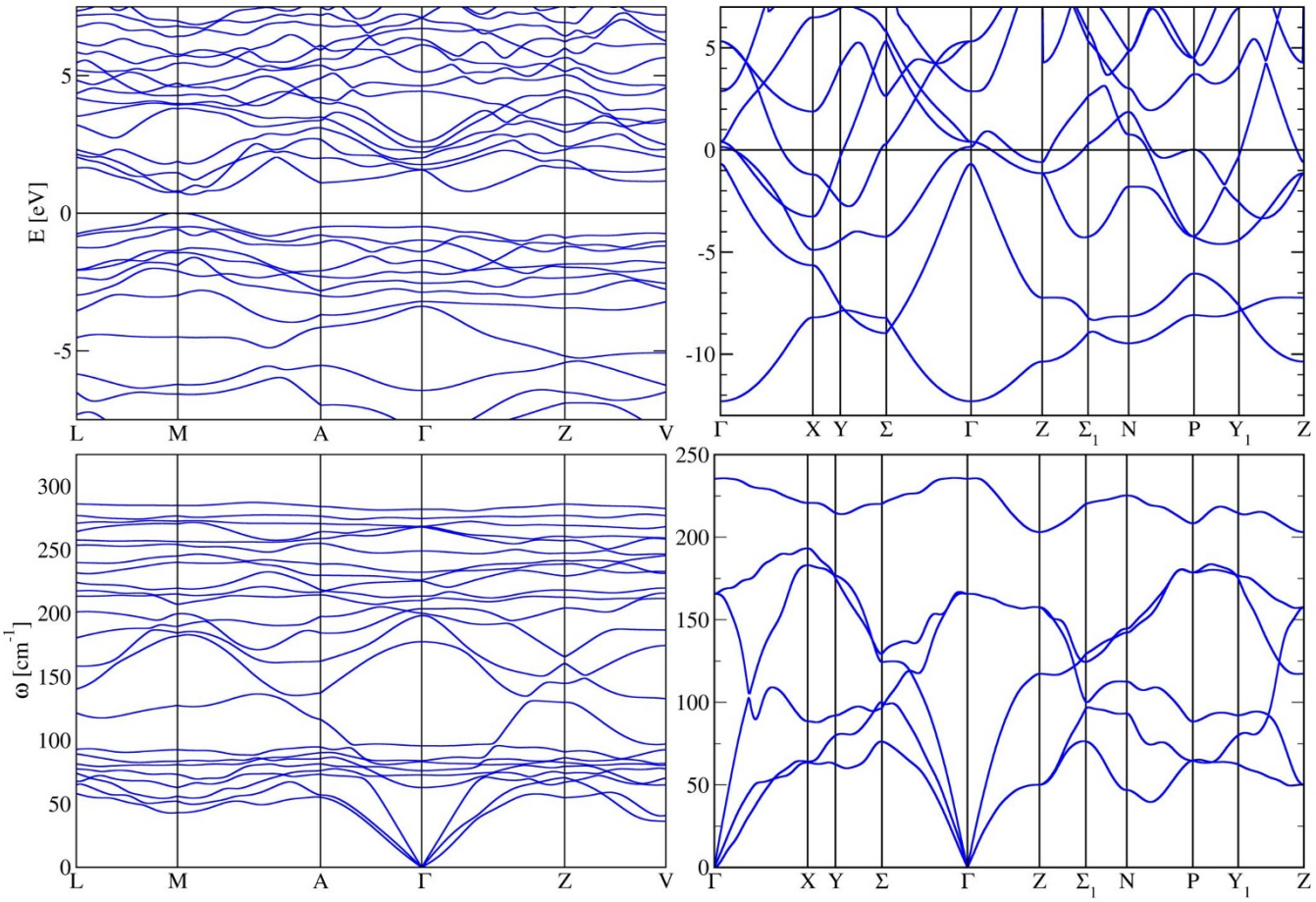

Figure 5 | Band structures and phonon spectra[23] (0.0 GPa) of mC16 (left) and bct-5 (right). mC16 is a narrow-gap semiconductor (band gap = 1.43 eV), while bct-5 is metallic. Both are mechanically stable. Brillouin zone choice (bct-5) according to Ref. 24.

phases exist. Low-temperature nonequlibrium decompression further influences phase formation towards amorphous[21] and novel germaniums[22].

The transformation affects only one box parameter, suggesting nonhydrostatic shearing as the protocol of choice towards bct-5, also supported by the magic-stress approach which led to bct-5 in silicon[19]. Alternatively, low-temperature compression may be considered. The evolution of the enthalpy profile of metadynamics runs from diamond Ge (Fig. 3) shows bct-5 as a narrow plateau around metastep 160. Metadynamics runs started from bct-5 (Fig. 3, black curve) confirms it as a proper intermediate along the transition, which can be quenched down to room pressure, and which is mechanically stable (see below). Mechanistically, the coordination number increases from 4 to 5 on shortening one bond, followed by flattening of the pristine tetrahedron and formation of the square pyramidal geometry of bct-5, Fig. 3b. The four bonds in the pyramid basis are 2.62 Å long, the axial one 2.48 Å.

The evolution of the bonding situation from Ge diamond to β-tin over bct-5 is shown in Fig. 4. Calculation of the ELF[25] shows four, one + four and two + four bond attractors, respectively. The five "bonds" in this orbital-deficient, electron-deficient metallic bct-5 result from the *sp* Ge valence shell. This bonding scenario is reminiscent of the recently discovered superconducting Zintl phase $CaGe_3$[26], isosymmetric with bct-5.

The electronic band structures and phonon dispersions of mC16 and bct-5 are shown in Fig. 5. The tetrahedral mC16 phase is semiconducting with an indirect band gap of 1.43 eV (PBE-GGA[27]), while bct-5 is metallic and stable down to 0 GPa. Isothermic-Isobaric molecular dynamics (1 bar, 300 K, 2.5 ps) confirmed the stability of bct-5. mC16 is characteristic due to the presence of four-membered rings. However, this does not imply overall structure destabilization[28]. The expectation of a strained geometry is in fact not supported by total energy calculations, which place mC16 among the energetically lowest Ge allotropes. The indirect band gap and the low density (compared to the diamond type) make this germanium an attractive material. The need for a "negative" pressure makes a chemical path plausible.

Discussion

The prominent property of bct-5 is the conservation of metallic character down to ambient conditions. Calculations and experiments have shown an increase of the superconducting temperature on lowering pressure, with superconductivity still present at 6.9 GPa ($T_c \approx$ 6.0 K)[2], outside of the existence range of β-tin. This points to the existence of another superconducting phase. The evolution of T_c as a function of pressure for bct-5 and β-tin is shown in Fig. 6. The calculated value of T_c for bct-5 at 6.9 GPa is T_c = 6.1 K (β-tin T_c = 7.7 K). The ongoing debate on the feasibility of "strange" metals other than β-tin[2,9], and particularly the need for further explanations of the survival upon decompression of "metallic" metastable phases (not reliably identified as any known Ge phase up to now) open the door for a serious consideration of the role of the bct-5 in the lower pressure range, as a metallic state that qualifies for higher T_c values (via the McMillan relation).

In conclusion, with metadynamics runs we have found and characterized two novel Ge polymorphs. The first one, mC16, is an indirect gap semiconductor, and its structure is unprecedented for the tetrel family. The second bct-5 polymorph was suggested for Si. Our

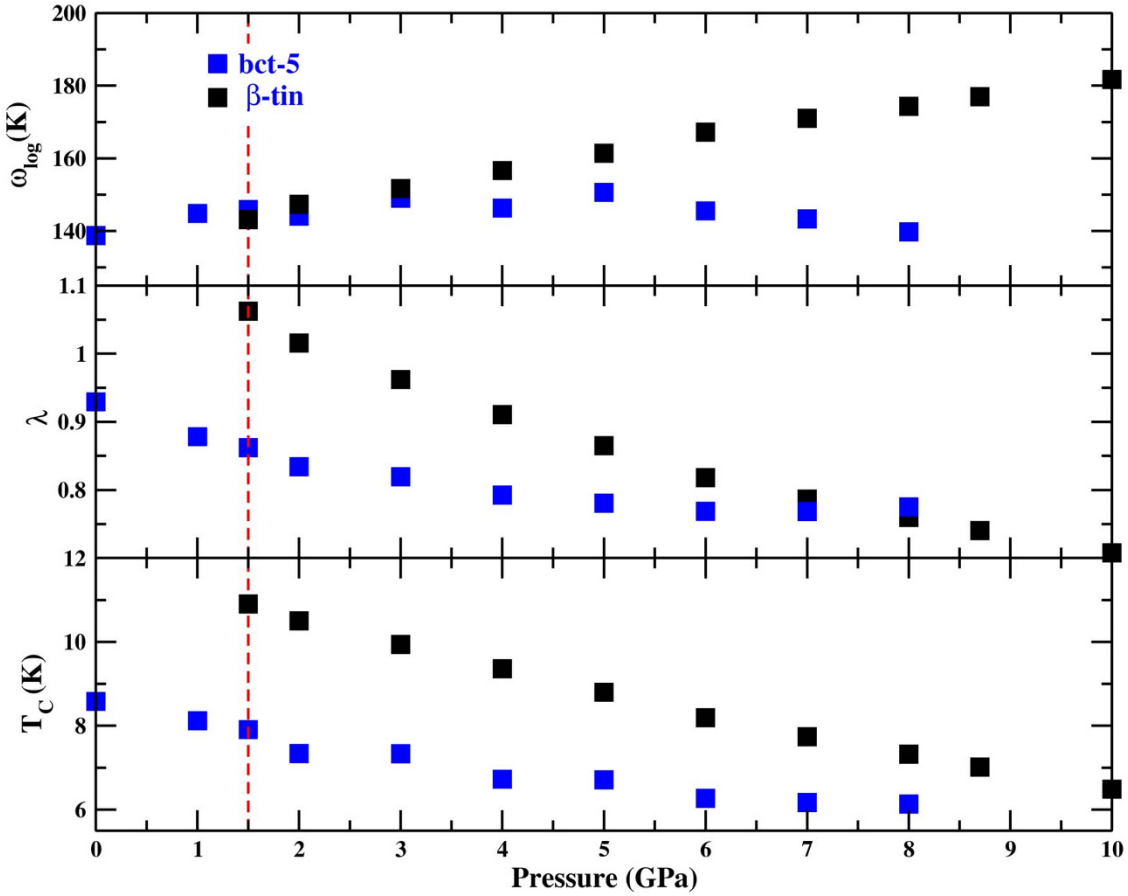

Figure 6 | Evolution of ω, λ and T_c as a function of pressure for bct-5 and β-tin, calculated based on the electron-phonon coupling model. The calculated equilibrium pressure between bct-5 and β-tin marks the boundary between the phases. Notice the flattening of bct-5 T_c after 5 GPa as phonons soften. The model predicts an increase of T_c in the lower pressure region.

simulations lean strong relevance to bct-5 in the lower pressure range, as a new metallic superconducting phase capable of stability at room conditions. We expect our predictions to stimulate further experimental work.

Methods

Metadynamics. Different approaches are successful in the prediction of novel polymorphs of the elements[29,30]. Important discoveries have been achieved by means of random techniques, genetic (evolutionary) algorithms, or accelerated molecular dynamics[10]. Metadynamics[31–33] allows for the exploration of the energy surface along one or more collective reaction coordinates. The method is independent of the level of theory used, it does not require prior knowledge of the energy landscape and its sampling efficiency can be enhanced by parallel runs started from different configurations. The time-evolution of the system is biased by a history-dependent potential, which discourages the system from visiting already harvested regions of the potential[34]. Efficiency is achieved in metadynamics also through dimensionality reduction. Instead of studying the problem in the full 3N dimensional configuration space of N particles, a relatively small number of collective coordinates $\mathbf{s} = (s_1..s_m)$ is used instead, which provide a coarse-grained description of the system and are able to distinguish between different free energy minima, i.e. different phases. The inclusion in the space of collective variables of slow degrees of freedom positively impacts the performance of the method.

All metadynamics runs were performed with at least eight atoms in the simulation box which served as a collective (6-dimensional) variable. This minimal box approach was successfully used in the prediction of novel carbon polymorphs, recently[7]. The size of the minimal box ensured commensurability of all already known phases (except for the clathrate II phase, which requires a minimum of 34 atoms) either open or dense. Each metadynamics metastep consisted of a molecular dynamics run in the NVT ensemble for 0.5 ps (timestep 2 fs) at 300 K.

Density functional computational layers. Metadynamics was performed with different molecular dynamics layers. A Density Functional Tight Binding (DFTB)[35] level of theory, as implemented in the Γ-point-only DFTB module of the CP2K code[36,37], ensured rapid and accurate sampling in the low-pressure regime, characterized by four-connected Ge atoms. For higher-pressures SIESTA[38] was used as the DFT molecular dynamics layer, allowing for k-point runs. Electronic states were expanded by a single-ζ basis set constituted of numerical orbitals with a norm-conserving Troullier-Martins[39] pseudopotential description of the core electrons. Single-ζ basis set dramatically reduces computational times providing nonetheless, the right topology and energy differences of all the Ge allotropes under study. The charge density was represented on a real-space grid with an energy cutoff[38] of 200 Ry. A Monkhorst-Pack k-point mesh of 2 × 2 × 2 ensured the convergence of the electronic part. High-pressure metadynamics was performed based on DFT. Lower pressure regions were initially explored by DFTB, followed by DFT metadynamics upon discovery of interesting novel polymorphs. In the lower pressure range the transferability between DFTB and DFT is unflawed. To validate the method a set of preliminary test runs were performed. Similarly to metadynamics applied to silicon[40], the correct sequence of reported phases[3] of Ge could be reproduced (not shown).

Band structures, phonons and electron-phonon coupling. Electronic structure, phonon dispersion curves and superconducting properties were calculated with the Quantum Espresso (QE)[20,23] package. The superconducting critical temperature T_c was evaluated based on the Allen and Dynes modification of the McMillan formula. This required calculating the electron-phonon coupling strength λ via the Eliashberg function. The Coulomb potential value was $\mu = 0.1$. A q-mesh of 12 × 12 × 12 was used for the evaluation of the dynamical matrix, while a Monkhorst-Pack k-point mesh of 16 × 16 × 16 ensured convergence of the electronic part.

Structure characterization. The structures visited during each run were characterized by their vertex symbols, which contain the information on all the shortest rings meeting at each atom, and coordination sequences, as implemented in the TOPOS package[41]. In case of new structures ideal space group and asymmetric units were identified with the Gavrog Systre package[42]. Subsequently a variable-cell geometry optimization was performed (DFT-GGA, PBE functional[27]) in a plane-wave pseudopotential framework[23] using Vanderbilt ultrasoft pseudopotential with non-linear core correction[43]. A k-point mesh of 8 × 8 × 8 ensured convergence of the electronic part, while a plane-wave basis set with an energy cut-off of 30 Ry was applied.

Electron localization function. The electron localization function (ELF)[25] is a widely used tool to study chemical bonding in molecules and solids. The ELF monitors the

correlation of the movement of parallel spin electrons in real space[44]. In this study the ELF calculations were performed by using the ELF module as implemented[45] in the all-electron, full-potential local orbital (FPLO) minimal basis method[46]. In FPLO each atomic orbital nl with principal quantum number n and angular momentum l is represented by one basis function only. The basis functions are obtained by solving an effective Schrödinger equation which contains the spherically averaged crystal potential and an artificial confining potential[47]. The confining potential makes the basis functions more localized than the atomic orbitals. The FPLO method does not have any atomic (or muffintin) spheres so that the whole space is treated in a uniform manner. In the scalar relativistic calculations within the LDA scheme (Perdew and Wang[48]) Ge(3d, 4s, 4p, 4d) represented the basis sets. Lower-lying states were treated as core states.

1. Mujica, A., Rubio, A., Munoz, A. & Needs, R. High-pressure phases of group-IV, III-V, and II-VI compounds. *Rev. Mod. Phys.* **75**, 863–912 (2003).
2. Cui, H. B., Graf, D., Brooks, J. S. & Kobayashi, H. Pressure-dependent metallic and superconducting phases in a germanium artificial metal. *Phys. Rev. Lett.* **102**, 237001 (2009).
3. Chen, X.-J. *et al.* β-tin→Imma→sh phase transitions of germanium. *Phys. Rev. Lett.* **106**, 135502 (2011).
4. Schwarz, U. Metallic high-pressure modifications of main group elements. *Z. Kristallogr.* **219**, 376–390 (2004).
5. Katzke, H. & Tolédano, P. Structural mechanisms of the high-pressure phase transitions in the elements of group IVa. *J. Phys-Condens. Mat.* **19**, 275204 (2007).
6. Oganov, A. R. & Glass, C. W. Crystal structure prediction using ab initio evolutionary techniques: principles and applications. *J. Chem. Phys.* **124**, 244704 (2006).
7. Selli, D., Baburin, I. A., Martoňák, R. & Leoni, S. Superhard sp(3) carbon allotropes with odd and even ring topologies. *Phys. Rev. B* **84**, R161411 (2011).
8. Claeys, C., Mitard, J., Eneman, G., Meuris, M. & Simon, E. Si versus Ge for future microelectronics. In *Thin Solid Films*, 2301–2306 (IMEC, B-3001 Louvain, Belgium, 2010).
9. Li, D., Ma, Y. & Yan, J. Comment on "Pressure-dependent metallic and superconducting phases in a germanium artificial metal" *Phys. Rev. Lett.* **104**, 139701; author reply 139702 (2010).
10. Oganov, A. R. *Modern Methods of Crystal Structure Prediction* (Wiley-VCH, 2011).
11. Lewis, S. & Cohen, M. Prediction of an Orthorhombic Phase of Germanium. *Solid State Commun.* **89**, 483–486 (1994).
12. Menoni, C., Hu, J. & Spain, I. Germanium at high pressures. *Phys. Rev. B* **34**, 362–368 (1986).
13. Nelmes, R. *et al.* Imma phase of germanium at 80 GPa. *Phys. Rev. B* **53**, R2907–R2909 (1996).
14. Vohra, Y. *et al.* Phase-Transition Studies of Germanium to 1.25 Mbar. *Phys. Rev. Lett.* **56**, 1944–1947 (1986).
15. Takemura, K. *et al.* High-pressure Cmca and hcp phases of germanium. *Phys. Rev. B* **62**, R10604 (2000).
16. Schwarz, U. *et al.* A 3D Network of four-bonded germanium: A link between open and dense. *Angew. Chem. Int Ed. Engl* **47**, 6790–6793 (2008).
17. Guloy, A. M. *et al.* A guest-free germanium clathrate. *Nature* **443**, 320–323 (2006).
18. Nelmes, R., McMahon, M., Wright, N., Allan, D. & Loveday, J. Stability and crystal structure of BC8 germanium. *Phys. Rev. B* **48**, 9883–9886 (1993).
19. Boyer, L., Kaxiras, E., Feldman, J., Broughton, J. & Mehl, M. New low-energy crystal structure for silicon. *Phys. Rev. Lett.* **67**, 715–718 (1991).
20. Baroni, S., de Gironcoli, S., Dal Corso, A. & Giannozzi, P. Phonons and related crystal properties from density-functional perturbation theory. *Rev. Mod. Phys.* **73**, 515–562 (2001).
21. Brazhkin, V. V., Lyapin, A. G., Popova, S. V. & Voloshin, R. N. Nonequilibrium phase transitions and amorphization in Si, Si/GaAs, Ge, and Ge/GaSb at the decompression of high-pressure phases. *Phys. Rev. B* **51**, 7549–7554 (1995).
22. Lyapin, A. G., Brazhkin, V. V., Popova, S. V. & Sapelkin, A. V. Nonequilibrium phase transformations in diamond and zincblende semiconductors under high pressure. *Phys. Stat. Sol. B* **198**, 481–490 (1996).
23. Giannozzi, P. *et al.* QUANTUM ESPRESSO: a modular and open-source software project for quantum simulations of materials. *J. Phys-Condens. Mat.* **21**, 395502 (2009).
24. Setyawan, W. & Curtarolo, S. High-throughput electronic band structure calculations: Challenges and tools. *Computational Materials Science* **49**, 299–312 (2010).
25. Becke, A. D. & Edegecombe, K. E. A Simple Measure of Electron Localization in Atomic and Molecular-Systems. *J. Chem. Phys.* **92**, 5397–5403 (1990).
26. Schnelle, W. *et al.* Dumbbells of five-connected Ge atoms and superconductivity in CaGe3. *Inorg. Chem.* **51**, 5509–5511 (2012).
27. Perdew, J., Burke, K. & Ernzerhof, M. Generalized gradient approximation made simple. *Phys. Rev. Lett.* **77**, 3865–3868 (1996).
28. Karttunen, A. J., Fässler, T. F., Linnolahti, M. & Pakkanen, T. A. Structural principles of semiconducting Group 14 clathrate frameworks. *Inorg. Chem.* **50**, 1733–1742 (2011).
29. Ma, Y. *et al.* Transparent dense sodium. *Nature* **458**, 182–186 (2009).
30. Oganov, A. R. *et al.* Ionic high-pressure form of elemental boron. *Nature* **457**, 863–867 (2009).
31. Martoňák, R. Atomistic simulations of pressure-induced structural transformations in solids. *Eur. Phys. J. B* **79**, 241252 (2011).
32. Martoňák, R., Laio, A. & Parrinello, M. Predicting crystal structures: the Parrinello-Rahman method revisited. *Phys. Rev. Lett.* **90**, 075503 (2003).
33. Martoňák, R., Donadio, D., Oganov, A. R. & Parrinello, M. Crystal structure transformations in SiO_2 from classical and ab initio metadynamics. *Nature Materials* **5**, 623–626 (2006).
34. Laio, A. & Gervasio, F. L. Metadynamics: a method to simulate rare events and reconstruct the free energy in biophysics, chemistry and material science. *Rep. Prog. Phys.* **71**, 126601 (2008).
35. Frauenheim, T. *et al.* A self-consistent charge density-functional based tight-binding method for predictive materials simulations in physics, chemistry and biology. *Phys. Status Solidi B* **217**, 41–62 (2000).
36. Lippert, G., Hutter, J. & Parrinello, M. A hybrid gaussian and plane wave density functional scheme. *Mol. Phys.* **92**, 477–488 (1997).
37. Lippert, G., Hutter, J. & Parrinello, M. The gaussian and augmented-plane-wave density functional method for ab initio molecular dynamics simulations. *Theor. Chem. Acc.* **130**, 124–140 (1999).
38. Soler, J. *et al.* The SIESTA method for ab initio order-N materials simulation. *J. Phys-Condens. Mat.* **14**, 2745–2779 (2002).
39. Troullier, N. & Martins, J. Efficient pseudopotentials for plane-wave calculations. *Phys. Rev. B* **43**, 1993–2006 (1991).
40. Behler, J., Martoňák, R., Donadio, D. & Parrinello, M. Metadynamics Simulations of the High-Pressure Phases of Silicon Employing a High-Dimensional Neural Network Potential. *Phys. Rev. Lett.* **100**, 185501 (2008).
41. Blatov, V. Multipurpose crystallochemical analysis with the program package TOPOS. *IUCr CompComm Newsletter* **7**, 4–38 (2006).
42. Delgado-Friedrichs, O. Generation, Analysis and Visualization of Reticular Ornaments. http://gavrog.org. Last accessed: 26.01.2013.
43. Vanderbilt, D. Soft self-consistent pseudopotentials in a generalized eigenvalue formalism. *Phys. Rev. B* **41**, 7892–7895 (1990).
44. Kohout, M. A measure of electron localizability. *Int. J. Quantum Chem.* **97**, 651–658 (2004).
45. Ormeci, A., Rosner, H., Wagner, F., Kohout, M. & Grin, Y. Electron localization function in full-potential representation for crystalline materials. *J. Phys. Chem. A* **110**, 1100–1105 (2006).
46. Koepernik, K. & Eschrig, H. Full-potential nonorthogonal local-orbital minimum-basis bandstructure scheme. *Phys. Rev. B* **59**, 1743–1757 (1999).
47. Eschrig, H. *Optimized LCAO Methods and the Electronic Structure of Extended Systems* (Springer, Berlin, 1989).
48. Perdew, J. & Wang, Y. Accurate and simple analytic representation of the electron-gas correlation energy. *Phys. Rev. B* **45**, 13244 (2002).

Acknowledgments

R.M. was supported by the Slovak Research and Development Agency under Contract No. APVV-0558-10 and by the project implementation 26220220004 within the Research & Development Operational Programme funded by the ERDF. S.L. thanks the DFG for support under the priority project SPP 1415, as well as ZIH Dresden for the generous allocation of computational resources. We acknowledge discussions with K. Syassen and E. Tosatti. We are thankful to Chris Pickard for deep insights into phonon calculations.

Author contributions

D.S., I.A.B., R.M. and S.L. designed research, performed simulations, analyzed data, and wrote the manuscript.

Additional information

Competing financial interests: The authors declare no competing financial interests.

License: This work is licensed under a Creative Commons Attribution-NonCommercial-NoDerivs 3.0 Unported License. To view a copy of this license, visit http://creativecommons.org/licenses/by-nc-nd/3.0/

How to cite this article: Selli, D., Baburin, I.A., Martoňák, R. & Leoni, S. Novel metastable metallic and semiconducting germaniums. *Sci. Rep.* **3**, 1466; DOI:10.1038/srep01466 (2013).